EFDA–JET–CP(10)05/07

G. Arnoux, B. Bazylev, M. Lehnen, A. Loarte, V. Riccardo, S. Bozhenkov, S. Devaux, T. Eich, W. Fundamenski, T. Hender, A. Hube, S. Jachmich, U. Kruezi, G. Sergienko, H. Thomsen and JET EFDA contributors

Heat Load Measurements on the JET First Wall during Disruptions

Heat Load Measurements on the JET First Wall during Disruptions

G. Arnoux[1*], B. Bazylev[2], M. Lehnen[3], A. Loarte[4], V. Riccardo[1], S. Bozhenkov[3], S. Devaux[5], T. Eich[5], W. Fundamenski[1], T. Hender[1], A. Huber[3], S. Jachmich[4], U. Kruezi[3], G. Sergienko[3], H. Thomsen[7] and JET EFDA contributors[*]

JET-EFDA, Culham Science Centre, OX14 3DB, Abingdon, UK

[1]EURATOM-UKAEA Fusion Association, Culham Science Centre, OX14 3DB, Abingdon, OXON, UK
[2]Forschungzentrum Karlsruhe GmbH, P.O.Box 3640, D-76021 Karlsruhe, Germany
[3]Institut für Energieforschung - Plasmaphysik, Forschungzentrum Jülich, Trilateral Euregio Cluster, EURATOM-Assoziation, D-52425 Jülich, Germany
[4]ITER organisation, Fusion Science and Technology Department, Cadarache, 13108 St Paul-Lez-Durance, France.
[5]Max-Planck-Institut für Plasmaphysik, EURATOM-Assoziation, D-85748 Garching, Germany
[6]Association EURATOM - Belgian State, Laboratory for Plasma Physics Koninklijke Militaire School - Ecole Royale Militaire Renaissancelaan 30 Avenue de la Renaissance B-1000 Brussels Belgium
[7]Max-Planck-Institut für Plasmaphysik, Teilinsitut Greifswald, EURATOM-Assoziation, D-17491 Greifswald, Germany
** See annex of F. Romanelli et al, "Overview of JET Results", (Proc. 22[nd] IAEA Fusion Energy Conference, Geneva, Switzerland (2008)).*

Preprint of Paper to be submitted for publication in Proceedings of the 19th International Conference on Plasma Surface Interactions, San Diego, California, USA. (24th May 2010 - 28th May 2010)

ABSTRACT

Disruptions in tokamaks lead to high heat loads onto the Plasma Facing Components PFC). Two processes, of particular concern for the first wall integrity, have been studied in dedicated experiments at JET: 1) During the thermal quench, it is measured (using fast IR thermography) that 5% of the plasma stored energy is deposited onto the outer and inner poloidal limiters. More surprisingly, during the current quench, about 10% of the magnetic energy is deposited onto the outer and inner poloidal limiters via plasma wall interaction. 2) Very localised heat loads due to runaway electrons, generated in disruptions triggered by massive injection of argon and neon, are measured onto the JET upper dump plate. The temperature increase is found to scale with the square of the runaway current.

1. INTRODUCTION

Disruptions in tokamaks lead to high heat loads onto the Plasma Facing Components (PFC). This is a great concern for the PFC life time of future fusion devices. In this paper, we focus on two particular mechanism: 1) The heat loads due to the thermal quench (TQ). 2) The heat load due to runaway electrons (RE).

During a disruption, the remaining stored energy, $W_{th,TQ}$, which is about 30% of that of a full performance plasma [1], is released in about 1ms (TQ). It was measured on JET that 10 to 50% of $W_{th,TQ}$ goes onto the divertor suggesting that 50 to 90% goes onto the first wall [2]. Characterising the heat load deposited onto the first wall provides some guidance for the design of future devices, such as ITER. Recent studies at JET showed that in high triangularity plasmas, part of $W_{th,TQ}$ is deposited onto the upper dump plate on a time scale 3 to 8 times longer than that of the plasma collapse. A broadening of the scrape-off layer was observed suggesting enhanced perpendicular transport [3]. We complete these results by characterising the heat loads onto the outer and inner limiters. Massive Gas Injection (MGI) is recognised as a good candidate to mitigate consequences of disruptions. It enhances radiation losses prior to the TQ, hence reduces the thermal energy lost during the TQ [4]. Whether it also mitigates heat loads during the TQ is discussed on the basis of heat loads measurements on the outer divertor target.

Following the TQ, the plasma current decays (current quench) rapidly, in first approximation as an exponential: $I_p \simeq I_0 \, exp\,\{t/\tau_{R/L}\}$, with typically $\tau_{R/L}$ = 7ms at JET. Part of the magnetic energy, $W_{mag} = 0{:}5LI_P^2$ with L = 5μH the total inductance and I_p the plasma current, is transferred to the first wall via radiation. The asymmetry of the radiation pattern can lead to high heat loads and is discussed in [5]. Runaway Electrons can also be generated (RE) that eventually are lost to the first wall [6]. The loss mechanism, associated with the end of the current plateau (see figure 2f) is not clearly understood. In ITER, for a 10MA RE beam current, the kinetic energy carried by the beam would be 20MJ whereas its magnetic energy would be 350MJ [7]. What fraction of the magnetic energy is dissipated into the first wall is a crucial question. The RE impact measured onto the JET upper dump plate by IR thermography provides a substantial information to tackle this question.

Measurements of heat loads during fast event such as the thermal quench or RE impacts requires a minimum time resolution of 1ms. In order to meet this requirement with the wide angle Infrared (IR) camera, Region Of Interests (ROI) must be selected. Examples of the ROI are shown in figure

1. This implies that good coverage of the PFC, with a fast time resolution can only be achieved in dedicated experiments. This restricts the number of measurements (1 key PFC per pulse) and makes statistical analysis too expensive.

2. HEAT LOADS DURING THERMAL QUENCH

Heat loads during the TQ were measured in a repeated scenario, where the ROI on the wide angle IR camera was changed on a pulse to pulse basis in order to cover the key PFC: the inner and outer poloidal limiters, and the upper dump plate (see figure coloured areas in 1). The toroidal magnetic field (B_t =2:1T) was ramped down until $q_{95} \simeq 2$ such that an MHD instability grows and triggers the disruption (a so called low q disruption). The heat load onto the outer divertor target (tile 5) was measured simultaneously with a high time (86μs) and space (2mm) resolution IR camera [8]. The surface temperature measurements are reduced to a 1D profile, T(*s, t*), where *s* is the poloidal distance along the PFC. For the limiters, the edge of the limiters only are selected (see white areas in figure 1) and T(*s, t*) is obtained by averaging the light intensity along the toroidal direction (approximately the vertical direction in the image). Heat load profiles, $q(s, t)$, are computed from $T(s, t)$ using the 2D, non-linear, finite elements code THEODOR [9] with, for the wall, the same thermal properties of the CFC as those used in [3].

Figure 2a summarises the scenario, showing the evolution of W_{th}, W_{mag} and W_{rad} 40 ms around the TQ (t=0), for the 5 JET pulses studied here (W_{rad} is the radiated energy measured by the bolometers [5]). Figure 2b shows the radial position of the plasma centre of mass, with respect to the major radius: $R(t)-R_0$. Figures 2c and d show the peak heat load on the inner, $q_{pk;in}(t) = \max_s \{q_{\mathrm{lim,in}}(s, t)\}$, and outer, $q_{pk;out} = \max_s \{q_{\mathrm{lim,out}}(s,t)\}$, limiters, and figure 2e shows the peak heat load on the outer target of the divertor (tile 5), $q_{pk;div}$;5. Defining the typical time scales: τ_{IR},in, $\tau_{\mathrm{IR,out}}$ and $\tau_{IR;div}$, as the time of the first maximum of $q_{pk;in}$, $q_{pk;out}$ and $q_{pk;div;5}$ after the thermal quench, one finds that $\tau_{IR;out}$ =1:2 ms, which is comparable to $t_{IR;div}$ = 0:86 ms and is on the time scale of the TQ, whereas $t_{IR;in} = 5ms$ is already in the CQ phase. However, at $t_{IR;out}$, both $q_{pk;in}$ and $q_{pk;out}$ have comparable values: about 15 MW/m^2. Given that the plasma moves inward, this is an indication of radial enhanced transport toward the low field side during the TQ. Both $q_{pk;out}$ and $q_{pk;in}$ reveal that substantial heat ($q_{pk} > 5$ MW/m^2) is deposited during the CQ for a period of 100 ms after the TQ. The heat load pattern, localised on the edge of the poloidal limiters, shows that the heat load is due to plasma wall interaction and not to radiation. Defining the total energy load onto the limiters as

$$W_{lim} = 2 \cdot N_{lim} \cdot e \int_{\Delta t} dt \int q(s, t) ds \tag{1}$$

where $N_{\mathrm{lim}} = 12$, is the number of limiters (for both inner and outer) and e = 50mm is the estimated width of the heat load pattern along the edge of the limiter, we can perform an energy balance. The factor 2 in (1) comes from the assumption that the two sides of each limiter take the same heat load, and toroidal symmetry is assumed such that each limiter take the same heat load. Table 1 shows the averaged energy load measured onto the divertor outer target, $W_{div;5}$, onto the wall, $W_{wall} = W_{lim;in} + W_{lim;out}$, and onto the upper dump plate, W_{dum}, normalised to $W_{th;TQ}$ and W_{mag} during the TQ and

the CQ respectively. Note that some PFC are not included, such as the ICRH antenna protection septums for example. W_{dum} and $W_{div;5}$ (see also [8, 10]) are calculated assuming toroidal symmetry such that:

$$W_{dum} = 2\pi \int_{\Delta t} dt \int R(s) q_{dum}(s, t) ds \tag{2}$$

$$W_{div} = 2\pi R_5 f_{wet} \int_{\Delta t} dt \int R(s) q_{div,\,5}(s, t) ds \tag{3}$$

where f_{wet} = 82% is the toroidal wetted area (it is a measured averaged value due to the fish skin like tile configuration) and R_5 is the averaged major radius at the position of tile 5. q_{dum} is calculated as in [3]. The end of the integration time interval, Δt, for the TQ, is defined at the peak of Ip so it guarantees that none of W_{mag} is included in the energy balance during the TQ. Δt for the CQ varies from one PFC to the other, from 15ms for$W_{div;5}$ and W_{dum} to 100ms for W_{wall}. From Table 1, one draws two main conclusions: 1) During the TQ, 65% of the thermal energy is radiated, while 11% is transported to the PFC, half of the conducted energy going to the wall. 2) During the CQ, more than 10% of W_{mag} is transfered to the PFC via plasma wall interaction (90MJ in 100ms), while half of it is radiated. Note that only one tile out of 8 is measured in the divertor, which can explain part of the missing energy in the balance during the TQ (25%). One other explanation is the error on the radiation measurement since Δt = 2:3 ms is on the limit of the time response of the bolometers. Note also that we assume toroidal symmetry, when MHD activity could break that symmetry, especially on the divertor [11]. Although incomplete, this energy balance gives a good idea of the distribution of the heat loads during the TQ. For the CQ, the missing energy is transferred to the magnetic coils and the vessel structure [12].

We investigated whether $W_{div;5}$, as defined in (2), during the TQ, is at all mitigated. 34 pulses have been investigated, including 6 low q disruptions as references. A wide range of $W_{th,TQ}$: 0.3 < $W_{th;TQ}$ < 3.4MJ was investigated, however for the low q disruptions, only the range: 0.5 ≤ $W_{th,TQ}$ ≤ 2.3 MJ was achieved. One measures that 2% ≤ W_{div} / $W_{th,TQ}$ ≤ 15%, the upper limit being measured for the low value of $W_{th,TQ}$ (< 1:5MJ) where a possible mitigation is observed. For $W_{th,TQ}$ >1.5 MJ, no clear distinction between MGI and non-MGI pulses (actually only one pulse), or between gas species can be made. Note that a large scatter in the reference measurements is observed, suggesting that the assumption of toroidal symmetry in the $W_{div;5}$ calculation may not be appropriate. These are preliminary results and further investigation are undergoing, including heat loads onto the first wall.

3. HEAT LOADS DUE TO RUNAWAY ELECTRONS

MGI has extensively been studied in JET and, when injecting argon, or neon, RE were observed [6]. Note that RE were not observed when a 90% D_2 and 10% Ar or Ne mixture was used. The hot (dark red) spots in the 5 white boxes shown in figure 1 (JPN76541), illustrate the distinct, localised impacts that have been measured on the upper dump plate. Identical footprints have been systematically observed on the 17 JET pulses selected for this study. It shows that the dump plate

geometry dominates the heat load distribution. Figure 2 shows the time evolution (JPN76541) 50 ms around the TQ of, I_p (f), the maximum surface temperature, T_i (g), of the 5 boxes (i = 1, ... ,5) and the 9 upper channels of the fast soft X-ray diagnostic (SXR) (h). The SXR measurement shows the RE beam building up [13] after the TQ for about 10ms before impacting the upper dump plate (when the series of spikes start). The impact coincides with the decay of the RE current plateau and with a large temperature increase (much larger than that of the TQ) on the upper dump plate. DTi systematically occurs within 2ms for i =1; ... ; 5. For i=5, a first temperature step is observed 2 ms earlier. Given that T5 is measured in a different poloidal position of the upper dump plate, this suggests an inward movement in the radial direction of the RE beam. Various RE beam current, I_{RE}, have been measured leading to different surface temperature rises. Here we define the RE beam current as the maximum departure from the exponential decay: $I_{RE} = \max_t \{I_{meas}(t) - I_{fit}(t)\}$ where $I_{fit}(t) = I_0 \exp\{t/\tau_R/L\}$ and I_{meas} is the current measurement. $\tau_{L/R}$ is evaluated on the first 3 ms of Imeas, well before the current plateau starts. Figure 3 shows a clear correlation between ΔT_{dum} and I_{RE}, where $\Delta T_{dum} = \Sigma^5_{i=1} \Delta T_i / 5$. The error bars show the minimum and maximum ΔT_i measured. Note that the maximum and minimum are not systematically observed on the same spot for each pulse. The trend followed by ΔT_{dum} suggests a power law:

$$\Delta T_{dum} = A \cdot I_{re}^{\alpha} \tag{4}$$

and the best fit gives $\alpha = 22 \pm 0.6$ with a rate of $A = 0{:}003\,^{o}\mathrm{C/kA}^2$. The error on α indicates the 95% interval of confidence on the fit. Modelling of the RE beam in a simplified geometry indicate that the corresponding energy density, Q_{RE}, is in the range: $0{:}5 \leq Q_{RE} \leq 3\mathrm{MJ/m}^2$ [14]. From this energy density, the current flowing into the CFC target has been calculated and good agreement is found with our measurements [14]. This indicates that I_{RE} as defined in this paper is a good measurement of the total energy (kinetic + magnetic) deposited by the RE beam into the first wall.

ACKNOWLEDGEMENT

This work was funded jointly by the United Kingdom Engineering and Physical Science Research Council and by the European Committee under the contract of Association between EURATOM and CCFE. The view and opinions expressed herein do not necessarily reflect those of the European Commission.

REFERENCES

[1]. V. Riccardo et al. Nuclear Fusion, **45**, 2005.
[2]. J. Paley et al. Journal Nuclear Material, 2005.
[3]. G. Arnoux et al. Nuclear Fusion, **49**, 2009.
[4]. M. Lehnen et al. Proc. in 36th EPS conference on Plasma Physics and Controlled Fusion, Sofia, 2009.
[5]. A. Huber et al. This conference, 2010.
[6]. M. Lehnen et al. Journal Nuclear Material, 2009.

[7]. A. Loarte. Private communication, 2009.
[8]. T. Eich et al. This conference, 2010.
[9]. A. Herrmann et al. Plasma Physics Controled Fusion, **37**:17–29, 1995.
[10]. H. Thomsen et al. This conference, 2010.
[11]. E. Nardon et al. This conference, 2010.
[12]. V. Riccardo et al. Plasma Physics Controled Fusion, **44**, 2002.
[13]. R.D. Gill et al. Nuclear Fusion, **40**, 2000.
[14]. B Bazylev et al. This conference, 2010.

	W_{rad}	W_{div}	W_{wall}	W_{dum}	Δt [ms]
TQ	56%	7%	4%	1%	2.3
CQ	46%	3%	9%	4%	15 – 100

Table 1. Radiated energy, W_{rad}, and energy load onto the divertor outer target, W_{div}, the poloidal limiters, W_{wall}, and the upper dump plate, normalised to the thermal energy, W_{th}, for the TQ, and to the magnetic energy, W_{mag}, for the CQ. Δt indicates the time interval over which the power load was integrated.

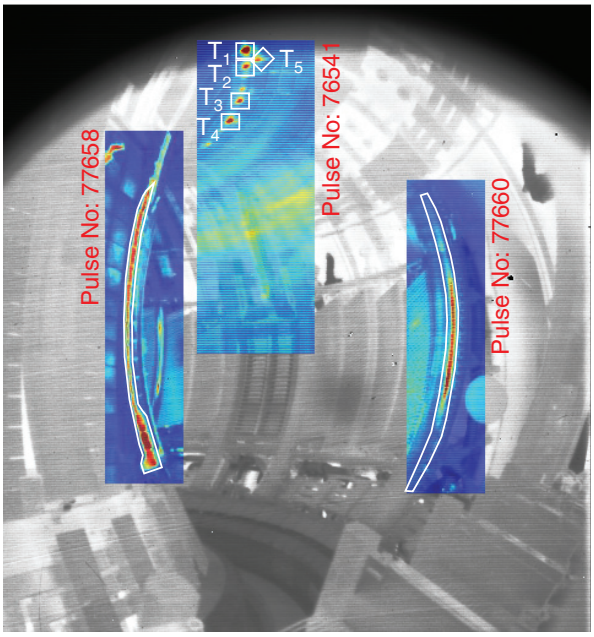

Figure 1: Plasma facing components as seen by the wide angle view infrared camera. The coloured areas are examples illustrating the ROI selected for fast time resolution measurement (1ms) onto key PFCs: the upper dump plate (JET Pulse No: 76541), the inner limiter (JET Pulse No: 77658) and the outer limiter (JET Pulse No: 77660).

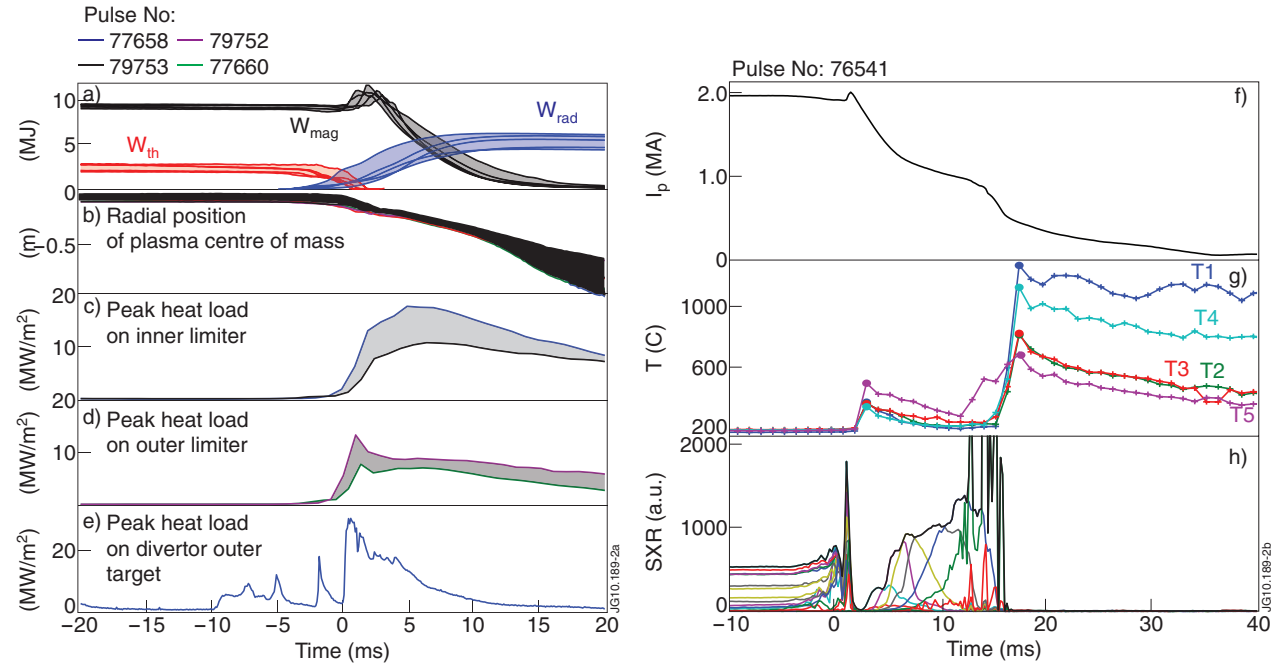

Figure 2: (a) the thermal, W_{th}, magnetic, W_{mag} and radiated, W_{rad} energies during the 40ms around the TQ (t=0). (b) the radial position of the centre of mass of the plasma with respect to the major radius, R_0. (c) to (e) the peak heat load measured on the inner limiter, outer limiter and outer target of the divertor respectively. (f) to (g), the plasm current, I_p, the temperatures, T1, ... ,T5 measured on the upper dump plate, and the soft X-ray channels, measured during an Ar-MGI disruption with the generation of a RE beam (I_{RE} =500 kA).

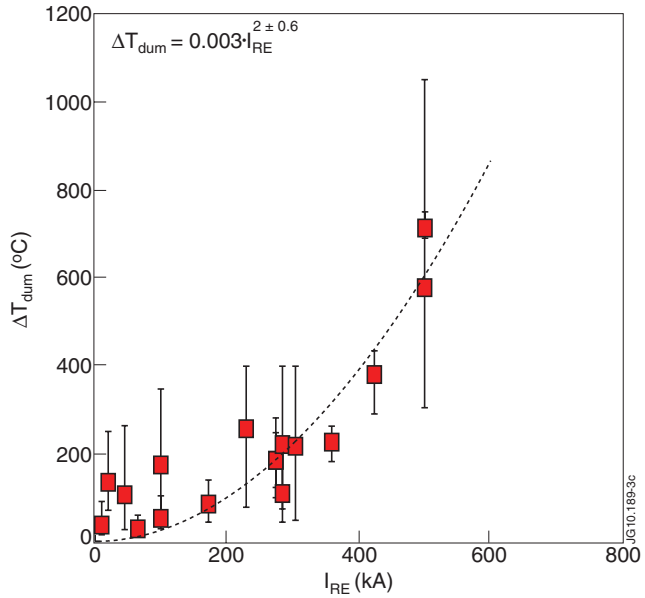

Figure 3: Averaged temperature increase measured on the JET upper dump plate due to RE impact as a function of the RE current. The averaging is made over the 5 different ROI shown in 1, each individual measurement, T_i, being the maximum temperature over the ROIs. The error bars denote the temperature range measured over the 5 ROIs.